

Topological Quantum Critical Points and Collective Modes of Fermi Gas in Non-Abelian Honeycomb Optical Lattice

Fa-Di Sun, Xiao-Lu Yu, Shao-Jian Jiang, Heng Fan and W. M. Liu
*Beijing National Laboratory for Condensed Matter Physics,
 Institute of Physics, Chinese Academy of Sciences, Beijing 100190, China*
 (Dated: December 21, 2018)

Motivated by recent experiments carried out by Esslinger's group at ETH [arXiv:1111.5020], we developed the local effective field theories to describe the universal properties of the topological quantum critical points in non-Abelian honeycomb optical lattice. We find that the ETH experiments, which manipulate Dirac points by changing the lattice anisotropy, can be realized in adjusting synthetic non-Abelian gauge potentials. From the effective metric tensor, which is induced by non-Abelian gauge potentials, we have identified two different types of local effective field theories. In one effective field theory the Fermi surface is a Dirac point, the short range Hubbard-like interactions are irrelevant and the collective modes are all damped. In the other effective field theory the Fermi surface is a nodal line, where there emerge a dimension crossover which leads to the short range Hubbard-like interactions being marginal and the collective modes being undamped.

PACS numbers: 03.75.Ss, 67.85.Lm, 37.10.Jk

Introduction.— Much of the interest in ultracold atomic gases comes from their amazing tunability in experiment. A wide range of atomic physics and quantum optics technology provide unprecedented manipulation of a variety of intriguing quantum phenomena. Recently, based on the Berry phase [1] and its non-Abelian generalization [2], Spielman's group in NIST has successfully generated a synthetic external Abelian or non-Abelian gauge potential coupled to neutral atoms. Realization of non-Abelian gauge potential in quantum gases will open a new avenue in cold atom physics [3, 4], which also has deep connections with relativistic field theories simulated by optical lattice [5, 6] and cosmology [7].

Control of ultracold atoms in a honeycomb optical lattice attracts lots of experimental [8, 9] and theoretical interests recently[10]. In this Letter, motivated by very recent experiments about the occurrence of topological transitions by manipulating Dirac points with a Fermi gas in a tunable honeycomb optical lattice [9], we will provide a general strategy for studying quantum criticality of non-Abelian honeycomb optical lattice. In the situation of no interactions, this problem has been partially studied in Ref. [11]. Starting from microscopic model, we identify topological quantum critical points (TQCPs) from corresponding energy spectrums by exactly solving the tight-binding model. At these TQCPs, we can develop local effective field theories (EFTs) to capture the interplay of non-Abelian gauge potential and atom-atom interaction. The essence of non-Abelian gauge potential is to provide the effective metric on the manifold of quantum vacuum, which setups a topological background for interaction effects.

Most importantly, two different types of quantum criticality will emerge at different quasi-momentum points, which can be unified and classified clearly within EFT. With different quantum scaling behavior, we will argue

the success of the tight-binding model and discuss how to observe experimentally these quantum critical behaviors. We also study collective modes on the honeycomb lattice with synthetic SU(2) gauge potential. Our work shows not only the manipulatable topological structure in ultracold Fermi gas systems with a non-Abelian honeycomb lattice experimentally, but also the EFT framework for quantum criticality of cold atom systems.

Energy spectrum and topological quantum critical points.— To study Fermi gas in two-dimensional (2D) honeycomb optical lattice with non-Abelian gauge potentials, we use the tight-binding model

$$\mathcal{H}_0 = -t \sum_{\langle i,j \rangle} U_{\sigma\sigma'}^\delta c_\bullet^\dagger(i\sigma') c_\circ(j\sigma) + h.c., \quad (1)$$

where t is hopping amplitude, $\langle i,j \rangle$ means the nearest neighbors, and $c_\bullet^\dagger(i\sigma), c_\circ^\dagger(i\sigma)$ ($c_\bullet(i\sigma), c_\circ(i\sigma)$) create (annihilate) an fermion at site \mathbf{r}_i of \bullet - and \circ -sublattice with spin σ . Tunneling operator U , which is a unitary operator, is related to non-Abelian gauge potentials \mathbf{A} by Schwinger line integral along the hopping path $\mathcal{P} \exp(i\frac{e}{\hbar} \int \mathbf{A} \cdot d\mathbf{l})$ [12]. In quasi-momentum space Eq. (1) becomes

$$\mathcal{H}_0 = -t \sum_{k\sigma\sigma'} c_\bullet^\dagger(k\sigma) \left(\sum_{\delta} U_{\sigma\sigma'}^\delta e^{ik\delta} \right) c_\circ(k\sigma') + h.c.. \quad (2)$$

In order to make the problem analytically tractable, we choose the gauge potentials on each hopping direction with the specific SU(2) form $U_1 = e^{i\alpha\sigma_x}$, $U_2 = I$ and $U_3 = e^{i\beta\sigma_y}$ [11]. Here α and β are adjustable parameters, (σ_x, σ_y) are Pauli matrices in the spin-components, $U_{1,2,3}$ are illustrated in Fig. 1. Then atoms hopping around an elementary plaquette is just a unitary transformation $U_{\square} = U_1 U_2 U_3 U_1^\dagger U_2^\dagger U_3^\dagger$, which describes the intrinsic symmetry of the spins for the fermions. By taking

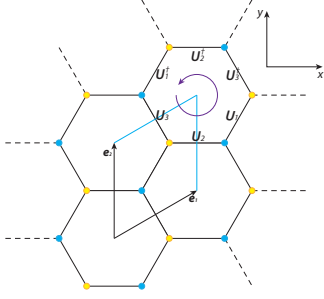


FIG. 1. (Color online) Bipartite honeycomb lattice can be considered as comprises of two triangular lattices, ●, denoted by dark blue dots and ○, denoted by light yellow dots.

TABLE I. Zero modes obtained from energy spectrum. We only list a half of them due to the time revers symmetry. In unit a^{-1} , a is the lattice spacing.

β	location of zero modes in moment space
$(0, \frac{\pi}{3})$	$(-\frac{1}{2} \arccos(\frac{-1+2\cos\beta}{2}) + \frac{2\pi}{3}, -\frac{1}{2\sqrt{3}} \arccos(\frac{-1+2\cos\beta}{2}))$ $(-\frac{1}{2} \arccos(\frac{-1+2\cos\beta}{2}) + \frac{\pi}{3}, -\frac{1}{2\sqrt{3}} \arccos(\frac{-1+2\cos\beta}{2}) + \frac{\pi}{\sqrt{3}})$
$(\frac{\pi}{3}, \frac{2\pi}{3})$	$(-\frac{1}{2} \arccos(\frac{-1+2\cos\beta}{2}) + \frac{2\pi}{3}, -\frac{1}{2\sqrt{3}} \arccos(\frac{-1+2\cos\beta}{2}))$ $(-\frac{1}{2} \arccos(\frac{-1+2\cos\beta}{2}) + \frac{\pi}{3}, -\frac{1}{2\sqrt{3}} \arccos(\frac{-1+2\cos\beta}{2}) + \frac{\pi}{\sqrt{3}})$ $(\arccos(\frac{\sqrt{1-2\cos\beta}}{2}), \frac{\sqrt{3}}{3} \arccos(\frac{\sqrt{1-2\cos\beta}}{2}))$ $(\arccos(-\frac{\sqrt{1-2\cos\beta}}{2}), \frac{\sqrt{3}}{3} \arccos(-\frac{\sqrt{1-2\cos\beta}}{2}))$
$(\frac{2\pi}{3}, \pi)$	$(\arccos(\frac{\sqrt{1-2\cos\beta}}{2}), \frac{\sqrt{3}}{3} \arccos(\frac{\sqrt{1-2\cos\beta}}{2}))$ $(\arccos(-\frac{\sqrt{1-2\cos\beta}}{2}), \frac{\sqrt{3}}{3} \arccos(-\frac{\sqrt{1-2\cos\beta}}{2}))$

trace of this unitary matrices, we can obtain the gauge-invariant Wilson loop $\mathcal{W} = \text{Tr} U_{\square} = 2 - 4 \sin^2 \alpha \sin^2 \beta$. The Wilson loop characterizes the non-Abelian magnetic flux through an elementary plaquette, which is non-local observable. We fix $\alpha = \pi/2$ and vary $\beta \in [0, \pi]$ to make expressions simple. The spectrum of \mathcal{H}_0 consists of four bands given by

$$\epsilon_{1\pm}(\mathbf{k}) = \pm t \sqrt{b - 2\sqrt{d}}, \quad \epsilon_{2\pm}(\mathbf{k}) = \pm t \sqrt{b + 2\sqrt{d}} \quad (3)$$

with $b = 3 + 2 \cos k_x \cos \beta$, $d = (\sin \sqrt{3} k_y - \cos \beta \sin k_x)^2 + \sin^2 \beta (1 - \cos 3k_x \cos \sqrt{3} k_y)$ and $k_{\pm} = 3/2 k_x \pm \sqrt{3}/2 k_y$. The spectrum is particle-hole symmetric, where ϵ_1 describes low-energy bands and ϵ_2 describes the higher-energy bands.

By solving $\epsilon_{1+}(\mathbf{k}) = 0$ for \mathbf{k} , we can obtain zero modes in analytic form which are listed in Table I. Obviously, varying β from 0 to π , we can find two types of merging of Dirac points, the corresponding critical points are $\beta = \pi/3$ and $\beta = 2\pi/3$. Explicitly, when $\beta \in (0, \pi/3)$, we have $N_D = 4$ massless Dirac zero modes; when $\beta \in (\pi/3, 2\pi/3)$, we have $N_D = 8$ massless Dirac zero modes; when $\beta \in (2\pi/3, \pi)$, we have $N_D = 4$ massless Dirac zero modes.

Varying configuration of gauge potentials, the system undergoes a topological quantum phase transition

(TQPT). Fermi surface is a topologically stable singularity of the Green function in moment space. TQPTs are induced by changes in Fermi-surface topology, so they are beyond Landau's paradigm [13]. The different phases in TQPTs are not classified by different symmetries, but characterized by different topologies of Fermi surface. Here these phases are defined by numbers of Dirac zero modes N_D . The TQPT is from $N_D = 8$ phase to $N_D = 4$ phase. Topological quantum phase transitions can be defined by the singularities of the ground-state energy as a function of the parameters in the Hamiltonian [14]. To get a better understanding of these singularities, we calculate the ground-state energy which is $\mathcal{E}(\beta) = \frac{1}{4\pi^2} \int_{BZ} d^2 \mathbf{k} (\epsilon_{1-}(\mathbf{k}) + \epsilon_{2-}(\mathbf{k}))$ where $\epsilon_{1,2-}(\mathbf{k})$ is given in Eq. (3) and BZ stand for the first Brillouin zone. We numerical calculate $\mathcal{E}(\beta)$ and its derivatives (Fig. 2). By checking this numerical result, we find that the second order derivative is continuous, but the third one has two discontinuous points. From those results, we can conclude that this phase transition is the third order TQPT, while in contrast, most conventional continuous quantum phase transitions are second order.

In order to have a close look of TQPT, we can calculate Berry phase for each Dirac point or equivalent winding number as the topological charge [15]. Examining these two critical points, we find this TQPT is due to merging of two Dirac points (see Fig. 3). These two Dirac points have opposite Berry phase, one is $+\pi$ and the other is $-\pi$. This type of TQPT can be interpreted as pair production or annihilation of Dirac modes.

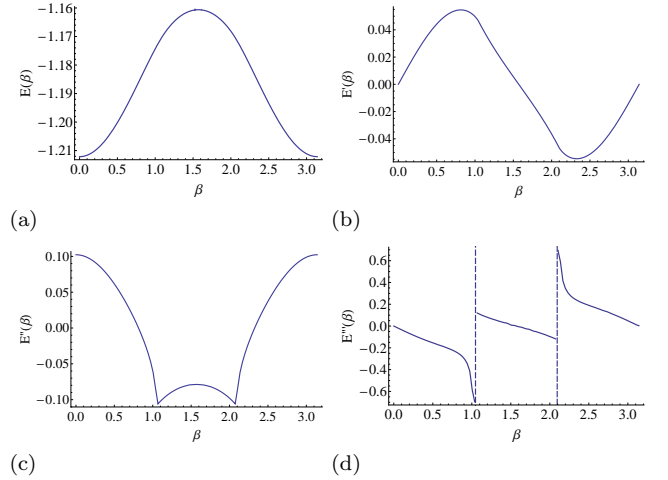


FIG. 2. (a) The ground-state energy and (b) its first-order derivative, (c) second-order derivative, and (d) third-order derivative. We can see that the first-order derivative and second-order derivative of the ground-state energy are continuous, while the third-order derivative begins to develop discontinuous.

Local effective field theory.— In what follows, we shall study local effective field theory at the TQCP, i.e. $\beta = \pi/3$. The 4×4 Hamiltonian \mathcal{H}_0 contains information

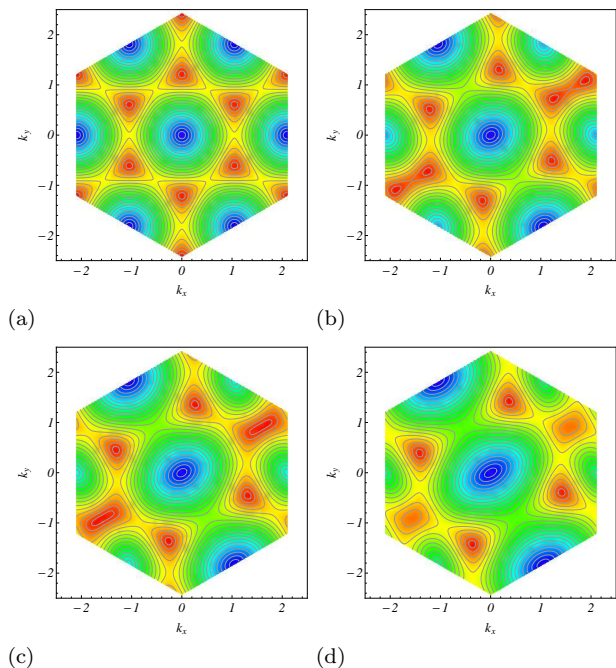


FIG. 3. (Color online) Counterplot of energy spectrum for non-Abelian gauge field configuration: (a) $\beta = \pi/2$, (b) $\beta = 2\pi/5$, (c) $\beta = \pi/3$ and (d) $\beta = \pi/4$. From (a) to (d), two pairs of Dirac points become close, then merge and finally disappear. The system undergoes a TQPT from $N_D = 8$ phase to $N_D = 4$ phase.

about the higher-energy band ϵ_2 , thus is not suitable to be described by a local effective field theory. At K point, which denote quasi-momentums of zero modes listed in Table I., we first find component for each bands by diagonalizing $\mathcal{H}_0(K)$. Then we can separate Hamiltonian into 2×2 blocks, and adiabatically eliminate higher-energy band contribution to get the effective two bands Hamiltonian. Now, we can expand Hamiltonian around the K point in terms of $k = K + q$ for $|q| \ll |K| \sim 1/a$. The small parameter, which governs the expansion of the energy dispersion, is, therefore, $|q|a \ll 1$. The continuum limit is reached by setting lattice spacing to approach zero; $\lim_{a \rightarrow 0} \mathcal{H}_0/a = \mathcal{H}_{\text{eff}}(\mathbf{k}) = T^{ij}k_i\sigma_j$. The square of the effective Hamiltonian then gives the space metric $g^{00} = -1, g^{0i} = 0, g^{ij} = T_{ik}T_{jk}$. It is easy to know that equal-energy surface is quadratic forms, discriminant can be expressed as $\Delta = -(\det T)^2$. Berry phase can be also obtained as $\text{sgn}(\det T)\pi$. So the significant character of our system is described by whether $\det T = 0$ or not. We find that T is nonsingular ($\det T \neq 0$) at $K_1 = (\frac{\pi}{2}, \frac{\pi}{2\sqrt{3}})$ point, singular ($\det T = 0$) at $K_2 = (\frac{5\pi}{12}, -\frac{\pi}{4\sqrt{3}})$ point. From the effective Hamiltonian we can construct local effective field theory at low energies as

$$\mathcal{S}_{\text{eff}} = \int d\omega d^2k \Psi_\mu^\dagger [\delta^{\mu\nu}\omega - T^{ij}k_i\sigma_j^{\mu\nu}] \Psi_\nu \quad (4)$$

The action can be viewed as zero density critical theory

[16, 17], which is our starting point to explore the interplay of non-Abelian gauge potential and atom-atom interaction.

Quantum scaling and collective modes.— In the following, we classify our local effective field theory by the determinant of T . There are two distinct cases:

(I) Dirac point ($\det T \neq 0$): When the matrix T becomes nonsingular, the Fermi surface is a point. Thus, the Fermi surface has codimension $d_c = 2$, which is defined as spatial dimension subtract dimension of Fermi surface [18]. The EFT is a massless “relativistic” Dirac theory. Now, we should scale the quasi-momentum as $d^2k \sim s^2 d^2k$ when rescaling of the energy $\omega \sim s\omega$, and the dimension of the fields will be $[\Psi] = -2$ in units of energy. Next we consider the influence of short-range interactions, which are mainly interactions in cold atom systems, i.e. Hubbard-like interactions. Fermionic renormalization group (RG) analysis shows that these interactions are irrelevant in weak coupling. This result can be also inferred from codimension of Fermi surface $d_c > 1$. As a consequence, weak short-range interactions should not affect too much the low energy properties. This lead to our conclusion that the single particle picture is reliable in weak coupling case. Things become complicated when interaction is strong coupling. Comparing with weak coupling case, in which we have a conventional semimetal with fermionic excitations at Dirac point, there might be an insulator with Néel order and some intermediate phases for strong coupling [17].

We can construct noninteracting Green function from effective action in Eq. (4)

$$\mathcal{G}^{(0)}(\mathbf{k}, i\omega_n) = [i\omega_n - \mathcal{H}(\mathbf{k})]^{-1} = \sum_{s=\pm} \frac{\mathcal{P}_s}{i\omega_n - s\epsilon_k} \quad (5)$$

where projector operators are defined as, $\mathcal{P}_s = \frac{1}{2}[\sigma_0 + sT_{ij}k_i\sigma_j/\epsilon_k]$, and $\epsilon_k = \sqrt{k_i T_{ik} T_{jk} k_j}$. The bare density and spin susceptibility can be expressed as,

$$\chi_{\mu\nu}(q, i\omega_n) = -k_B T \sum_{k, i\nu_n} \text{Tr}[\mathcal{G}^{(0)}(k+q, i\omega_n + i\nu_n)\sigma^\mu \times \mathcal{G}^{(0)}(k, i\nu_n)\sigma^\nu] \quad (6)$$

with $\sigma_\mu = (I, \boldsymbol{\sigma})$. For short-ranged Hubbard-like interactions, the random phase approximation (RPA) correction to the susceptibilities is given by $\chi^{\text{RPA}}(q, \omega + i\delta) = \chi[1 - U\Gamma\chi]^{-1}$ where Γ is a diagonal matrix $\text{diag}(1, -1)$ [19]. The collective mode for short-range interaction can be determined by the pole of χ^{RPA} , which is

$$-\frac{16v_{fx}v_{fy}}{V} = \left(1 + \frac{\omega^2}{v_{fx}^2q_x^2 + v_{fy}^2q_y^2}\right) \frac{v_{fx}^2q_x^2 + v_{fy}^2q_y^2}{\sqrt{v_{fx}^2q_x^2 + v_{fy}^2q_y^2 - \omega^2}} \quad (7)$$

where $v_{fx} = \sqrt{T_{11}^2 + T_{12}^2} \propto t$ and $v_{fy} = \sqrt{T_{21}^2 + T_{22}^2} \propto t$ after a proper frame rotation. It is obvious that there is

no real solution of ω for Eq.(7), so the collective modes are damped and do not propagate. Although hopping amplitude t and onsite interaction V are tunable in our case, we cannot obtain undamped collective mode at zero temperature in TQCP. Since these collective modes are damped in the wide region of parameter space, character stability Dirac excitation still dominates the low energy physics. In this case, our Dirac point has non-zero Berry phase $+\pi$ or $-\pi$, this non-zero Berry phase topologically protects the Dirac point. They are generally robust under weak perturbation which is different from the following case.

(II) Nodal line ($\det T = 0$): When the matrix T becomes singular, the Fermi surface is a straight line. Thus, the Fermi surface has codimension $d_c = 1$. We should scale the quasi-momentum as $d^2k \sim dk_{\parallel}sdk_{\perp}$ when rescaling of the energy $\omega \sim s\omega$, and the dimension of the fields would be $[\Psi] = -3/2$ in units of energy. Next we consider the influence of short-range interactions, which are mainly interactions in cold atom systems, i.e. Hubbard-like interactions. At the tree level, it is obvious that these interactions are marginal from RG theory of interacting fermions. So we need go further to the loop level to determine whether it is marginal relevant or marginal irrelevant. From the exact result of Yang and Yang [20], the RG flow of coupling constant stays zero to all orders, if the magnitude of original coupling strength is less than order unity. In this case, the corresponding energy spectrum becomes to $\epsilon(k) = \pm v_f k_x$, it is crucial to notice that our effective field theory depends on one direction only. We can make a dimension reduction and introduce the Hubbard-like interaction, then our 2D system can be viewed as a set of weakly coupled one dimensional (1D) spinless Luttinger Liquid in y -direction.

From Luttinger liquid theory[21], the dispersion of collective modes reads

$$\omega(q) = qv_f\sqrt{1 - V^2/V_c^2} \quad (8)$$

where $v_f = \sqrt{T_{11}^2 + T_{12}^2} \propto t$ after a proper frame rotation and critical interaction strength $V_c = 2\pi v_f$. Hopping amplitude t and onsite interaction V are all tunable parameters in the cold atom systems. If we tune them in the region $V > V_c$, our collective mode is damped. But V_c is so large that not reachable in current experiments, thus we cannot observe this damped mode. Moreover, reaching such a huge V_c large then the Fermi scale, the system becomes solid [22]. It is worthwhile emphasizing here that the solution is a non-perturbative result.

Nodal line comes from merging two Dirac points with opposite Berry phase, thus its effective Berry phase is zero. Nodal line is no longer topologically protected. Under weak perturbation, the nodal line may disappear. In some circumstances, nodal line disappears leaving behind the pairs of Fermi points. But in a more general case there is an alternative destiny for a nodal line: zeros can

disappear completely so that the system becomes local gapped [13].

Discussion and summary.— Very recently, Esslinger's group in ETH has successfully identified and manipulated Dirac points in the band structure by observing a minimum band gap inside the Brillouin zone via interband transitions with an ultracold Fermi gas of ^{40}K atoms in a two-dimensional tunable optical lattice [9]. The amazing tunability of their optical lattice structure allows for independent adjustment of the tunneling parameters along the different directions simply by controlling the intensity of the laser beams, which seems suitable to experimentally explore the new features of our case (I) EFT.

However, contrasted with case (I) EFT, the topological defect becomes unstable and the corresponding collective modes are undamped in our case (II) EFT. In high- T_c superconductor experiments, angle-resolved photoemission spectroscopy (ARPES) is a powerful tool to visualize the nodal line (point) defects. Although the technique of ARPES has not yet been realized in cold atom experiment, there is a very similar technique of momentum-resolved radio-frequency spectroscopy [23], which will be a promising tool to detect nodal line defects in ultracold Fermi gas. To further test the interaction effect on collective modes, one needs to have evidence for their linear dispersion relation dependence on the interaction strength, which is well tunable with the technique of Feshbach resonance. Ultimately, to make contact with experiments involving nodal line of ultracold fermions in a non-Abelian optical lattice, we must take into account the atom-atom interactions and attempt to determine the critical value of interaction strength V_c .

In summary, we construct a universal EFT to describe Fermi gas in a non-Abelian honeycomb lattice. This approach enable us to unify different universality class emerged from TQCPs and study their collective modes under the interplay of non-Abelian gauge potential and atom-atom interaction. We show that ETH experiments, which manipulate Dirac points by changing the lattice anisotropy, can be realized in adjusting non-Abelian gauge potentials. Our results are of particular significance both for manipulating topological structure in ultracold Fermi gas systems with a non-Abelian honeycomb lattice experimentally and for further studying quantum criticality of cold atom systems within the framework of EFT theoretically.

Acknowledgements.— We acknowledge insightful discussions with Carlos A. R. Sá de Melo and Alexei M. Tsvelik. This work was supported by NSFC under Grants No. 10934010 and No. 60978019, the NKBRSF under Grants No. 2009CB930701, No. 2010CB922904, No. 2011CB921502, and No. 2012CB821300, and NSFC-RGC under Grants No. 11061160490 and No. 1386-NHKU748/10.

-
- [1] M. V. Berry, Proc. R. Soc. Lond. A **392**, 45 (1984).
- [2] F. Wilczek and A. Zee, Phys. Rev. Lett. **52**, 2111 (1984).
- [3] Y.-J. Lin, R. L. Compton, A. R. Perry, W. D. Phillips, J. V. Porto, and I. B. Spielman, Phys. Rev. Lett. **102**, 130401 (2009); Y. J. Lin, R. L. Compton, K. Jimnez-Garca, J. V. Porto, and I. B. Spielman, Nature **462**, 628 (2009); Y.-J. Lin, R. L. Compton, K. Jiménez-García, W. D. Phillips, J. V. Porto, and I. B. Spielman, Nat. Phys. **7**, 531 (2011); Y.-J. Lin, K. Jimnez-Garca, and I. B. Spielman, Nature **471**, 83C86 (2011).
- [4] J. Dalibard, F. Gerbier, G. Juzeliūnas, and P. Öhberg, Rev. Mod. Phys. **83**, 1523 (2011).
- [5] A. Bermudez, L. Mazza, M. Rizzi, N. Goldman, M. Lewenstein, and M. A. Martin-Delgado, Phys. Rev. Lett. **105**, 190404 (2010).
- [6] L. Mazza, A. Bermudez, N. Goldman, M. Rizzi, M. A. Martin-Delgado, and M. Lewenstein, arXiv:1105.0932.
- [7] M. A. H. Vozmediano, M. I. Katsnelson, and F. Guinea, Physics Reports **496**, 109 (2010).
- [8] P. Soltan-Panahi, J. Struck, P. Hauke, A. Bick, W. Plenkers, G. Meineke, C. Becker, P. Windpassinger, M. Lewenstein, and K. Sengstock, Nature Physics **7**, 434 (2011).
- [9] L. Tarruell, D. Greif, T. Uehlinger, G. Jotzu, and T. Esslinger, arXiv:1111.5020.
- [10] S.-L. Zhu, B. Wang, and L.-M. Duan, Phys. Rev. Lett. **98**, 260402 (2007).
- [11] A. Bermudez, N. Goldman, A. Kubasiak, M. Lewenstein, and M. A. Martin-Delgado, New J. Phys. **12**, 033041 (2010).
- [12] T. T. Wu and C. N. Yang, Phys. Rev. D **12**, 3845 (1975).
- [13] G. E. Volovik, *The Universe in a Helium Droplet* (Oxford University Press, USA, 2003).
- [14] X. G. Wen, *Quantum Field Theory of Many-body Systems* (Oxford University Press, 2004).
- [15] X. Wen and A. Zee, Nuclear Physics B **316**, 641 (1989).
- [16] P. Nikolić and S. Sachdev, Phys. Rev. A **75**, 033608 (2007).
- [17] S. Sachdev, *Quantum Phase Transitions*, 2nd ed. (Cambridge University Press, 2011).
- [18] T. Senthil and R. Shankar, Phys. Rev. Lett. **102**, 046406 (2009).
- [19] S. Raghu, S. B. Chung, X.-L. Qi, and S.-C. Zhang, Phys. Rev. Lett. **104**, 116401 (2010).
- [20] C. N. Yang and C. P. Yang, Phys. Rev. **150**, 321 (1966).
- [21] T. Giamarchi, *Quantum Physics in One Dimension* (Oxford University Press, 2004).
- [22] P. W. Anderson, *Basic Notions Of Condensed Matter Physics (Advanced)* 2nd ed. (Westview Press / Addison-Wesley, 1997).
- [23] J. T. Stewart, J. P. Gaebler, and D. S. Jin, Nature **454**, 744 (2008).